Chapter 2

Death and Survival Signals in Photodynamic Therapy

Michael Dewaele, Tom Verfaillie, Wim Martinet, and Patrizia Agostinis

Abstract

Photodynamic therapy (PDT) is an anticancer modality utilizing the generation of singlet oxygen and other reactive oxygen species through visible light irradiation of a photosensitive dye accumulated in the cancerous tissue. Upon exposure of cancer cells to the photodynamic stress, multiple signaling cascades are concomitantly activated and depending on the subcellular location of the generated ROS and the intensity of the oxidative damage, they dictate whether cells will cope with the stress and survive or succumb and die. Different methodologies have been developed to allow the discrimination of cell death subroutines at the morphological, ultrastructural, and biochemical levels and to scrutinize signaling cascades in response to PDT. Here we describe a selection of useful techniques to characterize apoptosis and autophagy and to monitor the activation status of the MAPK- and Akt-mTOR pathways after PDT.

Key words: PDT, hypericin, signal transduction, protein kinases, apoptosis, autophagy, Odyssey.

1. Introduction

The present classification of cell death modalities, which includes apoptosis, autophagic cell death, and necrosis, is largely based on their distinguishable morphologies and biochemical hallmarks (1).

Apoptosis, or type 1 cell death, is regarded as the most widespread mode of cell death and is a major in vitro and in vivo response to PDT (2–4). Apoptosis is characterized by cell shrinkage, chromatin condensation and DNA fragmentation, membrane blebbing, activation of caspases, and, in vivo, phagocytosis by neighboring cells. In contrast, necrosis, also known as type 3 cell death, is characterized by cellular swelling, rapid loss

C.J. Gomer (ed.), *Photodynamic Therapy*, Methods in Molecular Biology 635,
DOI 10.1007/978-1-60761-697-9_2, © Springer Science+Business Media, LLC 2010

of plasma membrane integrity, and the absence of caspase signaling. This type of cell death occurs typically in response to excessive photodynamic injury to cellular components. During the last decades a number of techniques to discriminate apoptosis from necrosis have been extensively developed. These include measurements of DNA fragmentation, mitochondrial membrane permeabilization and release of mitochondrial intermembrane proteins in the cytosol, activation of caspases, and ultrastructural analysis of cell death morphologies by transmission electron microscopy. More recently, we and others have shown that PDT can activate autophagy which can result in an autophagic cell death, or type 2 cell death, which is morphologically defined (especially by transmission electron microscopy) as a type of cell death accompanied by large-scale autophagic vacuolization of the cytoplasm in the absence of chromatin condensation (4). Autophagy, literally "self-eating" in Greek, takes place at constitutively low levels in all eukaryotic cells as a main survival mechanism to maintain vital functions during nutrient-limiting conditions and to rid cells from aberrant or unnecessary organelles, toxic metabolites, or intracellular pathogens (5). Autophagy stimulation is observed under conditions of chronic metabolic stress, such as those found in the tumor microenvironment, as well as following acute damage to vital cellular components, as observed following a variety of anticancer treatments (6). The hallmark of autophagy is the formation of double-membraned vacuoles, called autophagosomes, that sequester cytoplasmic components as well as organelles, which eventually fuse with lysosomes to become a single-membraned autolysosome, where the cargo is degraded by lysosomal hydrolases. The detection and quantification of the autophagosomes present in the cells, the evaluation of the autophagic flux, and the activation status of signaling pathways regulating autophagy, such as the Akt-mTOR and the mitogen-activated protein kinases (MAPKs), are frequently used methods to analyze the stimulation of this catabolic process after cellular stress.

Because of the relevance of these signaling pathways in the regulation of the cell's fate, we describe here a selection of techniques used to monitor and characterize apoptotic cell death and autophagy and MAPK- and Akt-driven pathways in cell lines exposed to PDT.

2. Materials

2.1. Photosensitization and Cell Culture Media

1. Hypericin is synthesized from emodin anthraquinone according to Falk et al. (7), dissolved in dimethyl sulfoxide (DMSO) to attain 1,000X working stocks, and stored in dark conditions at –18°C.

2. Cell culture medium is prepared as follows: 500 ml DMEM (Dulbecco's Modified Eagle's Medium) supplemented with 100 units/ml penicillin, 100 μg/ml streptomycin, 2 mM L-glutamine (all from Gibco, Invitrogen, Carlsbad, CA, USA), and 10% (v/v) FBS (fetal bovine serum; HyClone, Thermo Fisher Scientific, Waltham, MA). This medium will be referred to as "serum-containing DMEM" in the protocols. After preparation store at 4°C.

2.2. Preparation of Protein Lysates

1. HEPES lysis buffer: 25 mM 4-(2-hydroxyethyl)-1-piperazine ethane sulfonic acid (HEPES) pH 7.5, 0.3 M NaCl, 1.5 mM $MgCl_2$, 20 mM β-glycerol-phosphate, 2 mM ethylenediaminetetraacetic acid (EDTA), 2 mM ethylene glycol tetraacetic acid (EGTA), 1 mM dithiothreitol (DTT), 1% (v/v) Triton X-100, 10% (v/v) glycerol, 10 μg/μl leupeptin, 5 μg/μl aprotinin, 1 mM phenyl methane sulphonyl fluoride (PMSF), 1 mM Na_3VO_4, and 50 mM NaF. Store aliquots at –18°C.

2.3. Gel Electrophoresis and Western Blotting

1. Determination of protein concentration: BCA™ protein assay kit (Pierce, Rockford, IL, USA).
2. 6X Loading buffer: 0.35 M Tris–HCl pH 6.8, 10% (w/v) SDS, 36% (v/v) glycerol, and 0.01% (w/v) bromophenol blue. Store aliquots at –20°C. For the aliquot in use, add 5% (v/v) β-mercaptoethanol.
3. TBS-T (Tris-buffered saline with Tween): 25 mM Tris–HCl pH 7.4, 150 mM NaCl, and 0.1% Tween. Store at RT.
4. Blocking buffer: 5% non-fat milk powder (Nestlé Belgilux NV, Brussels, Belgium) in TBS±T.
5. Secondary HRP-labeled antibody for ECL: Horse anti-mouse and goat anti-rabbit (Cell Signaling Technology, Danvers, MA, USA) diluted 1:2,000 in blocking buffer.
6. Secondary IR-labeled antibody for Odyssey: Alexa Fluor® 680 goat anti-rabbit IgG "highly cross-adsorbed" (Invitrogen, Carlsbad, CA, USA) diluted 1:5,000 in blocking buffer; DyLight 800 conjugated goat anti-mouse IgG (H+L) (Thermo Fisher Scientific, Rockford, IL, USA) diluted 1:5,000 in blocking buffer.

2.4. Assessment of Apoptosis in PDT-Treated Cells

2.4.1. Determination of Caspase Activity

1. Rabbit anti-caspase 3 (recognizing the proform and processed active forms) and mouse anti-poly(ADP-ribose) polymerase (PARP) recognizing the full protein and the caspase-cleaved PARP fragment (BIOMOL International LP, Plymouth Meeting, PA, USA).

2. Assay buffer: 100 mM HEPES pH 7.4, 10% (w/v) sucrose, 1% (v/v) Triton X-100, 2.5 mM EDTA, 5 mM DTT, 1 mM PMSF, 2 μg/ml pepstatin, and 2 μg/ml leupeptin. Store at 4°C.
3. Fluorescent substrates (7-amino-4-methylcoumarin (AMC)) and inhibitors (fluoromethyl ketone (FMK)) for the different caspases (Bachem GmbH, Weil am Rhein, Germany).

2.4.2. Determination of DNA Fragmentation by Sytox Green Staining

1. DNA extraction buffer: 0.2 M Na_2HPO_4 and 0.1 M nitric acid brought to pH 7.8 with NaOH.
2. DNA staining solution: 1 μM Sytox green (Invitrogen, Carlsbad, CA, USA) in PBS and 0.2 mg/ml DNase-free RNase.

2.4.3. Assessment of Mitochondrial Outer and Inner Membrane Permeabilization

1. Digitonin buffer: 0.01% (w/v) digitonin (Sigma-Aldrich, St. Louis, MO, USA) (stock solution: 1% in methanol, store at RT) and 1 mM EDTA diluted in PBS.
2. Stabilization buffer: 20 mM HEPES pH 7.5, 250 mM sucrose, 10 mM KCl, 1.5 mM $MgCl_2$, 1 mM EDTA, 1 mM EGTA, 1 mM DTT, 10 μg/ml leupeptin, 1 mM PMSF, and 10 μg/ml aprotinin.
3. Streptolysin O (Sigma-Aldrich, St. Louis, MO, USA).
4. Mouse anti-actin antibody (The Developmental Studies Hybridoma Bank, University of Iowa, Iowa City, IA, USA), mouse anti-cytochrome oxidase subunit IV antibody (Molecular Probes, Invitrogen, Carlsbad, CA, USA), and mouse anti-cytochrome *c* antibody (BD Biosciences, Franklin Lakes, NJ, USA).
5. DiOC6(3) (3,3′-dihexyl oxacarbocyanine iodide; Molecular Probes, Invitrogen, Carlsbad, CA, USA).

2.5. Transmission Electron Microscopy (TEM) for the Study of Cell Death

1. 0.033 M veronal acetate buffer: This buffer is prepared as follows. First, a veronal acetate stock solution is prepared by dissolving 9.71 g sodium acetate trihydrate and 14.71 g sodium 5,5-diethylbarbiturate in 500 ml ultrapure water. The veronal acetate stock solution can be stored for several weeks at 4°C. Subsequently, 6 g saccharose is dissolved in a small volume of water. After addition of 20 ml veronal acetate stock, the pH is adjusted to 7.2–7.4 using acetic acid. The solution is made up to 100 ml with ultrapure water, yielding 6% saccharose in 0.05 M veronal acetate buffer. Finally, two volumes of the latter buffer, 0.5 volume of 6% OsO_4, and 0.5 volume of water are mixed to obtain 0.033 M of veronal acetate buffer-containing 4% saccharose.
2. Reynolds solution: First, slightly heat (and stir) 17.6% sodium citrate. Slowly add 13.3% lead nitrate and leave

for 30 min at room temperature. Adjust to pH 10.5 with sodium hydroxide Titrisol. This stock solution can be stored at room temperature for several weeks. Prior to use, adjust to pH 12.4 with sodium hydroxide Titrisol. This pH is critical as pH > 12.45 will lead to precipitation whereas pH < 12.35 will give poor staining.

2.6. Monitoring Autophagy

1. Mouse anti-LC3 antibody (NanoTools, Antikörpertechnik GmbH & Co, Teningen, Germany).
2. pBABE-GFP-LC3 vector (Dr. J. Debnath, Dept. Cell Biology, Harvard Medical School, Boston, MA, USA).
3. Bafilomycin A1 (Sigma-Aldrich, St. Louis, MO, USA) is dissolved in DMSO to attain a 1,000X stock solution of 100 μM.

2.7. Monitoring MAPK and Akt-mTOR Signaling Cascades

1. Stripping buffer: 62.5 mM Tris–HCl pH 6.7, 2% (w/v) sodium dodecyl sulfate (SDS), and 100 mM β-mercaptoethanol (BME).
2. Mouse anti-p38 MAPK antibody; rabbit anti-phospho-p38 (Thr180/Tyr182) antibody; rabbit anti-Akt antibody; mouse anti-phospho-Akt (Ser473) antibody; rabbit anti-p70S6 antibody; mouse anti-phospho-p70S6 (Thr389) antibody; mouse anti-S6 ribosomal protein antibody; and rabbit anti-phospho-S6 ribosomal protein (Ser235/236) antibody (Cell Signaling Technology, Danvers, MA, USA) diluted 1:1,000 in blocking buffer; rabbit anti-JNK1 antibody was prepared as described in (8); rabbit anti-phospho-JNK 1 and 2 (Thr183/Tyr185) antibody (BioSource^{TM}, Invitrogen, Camarillo, CA, USA) diluted 1:1,000 in blocking buffer.

3. Methods

Here we describe a compendium of different techniques that are used to assess morphological and biochemical hallmarks of apoptosis, autophagy, and regulation of MAPK and Akt-mTOR signaling pathways after cell photosensitization (PDT). At the beginning of the different subchapters we will provide background, step-by-step protocols, and applications and discuss some alternative techniques which can be applied. Since the variety of photosensitizers used in PDT cannot be completely covered, we will focus on the photodynamic effects evoked by light activation of the naturally occurring photosensitizer hypericin, which upon cellular uptake has been shown to localize predominantly to the ER compartment (9, 10).

3.1. Photosensitization (PDT)

1. Seed cells to attain a confluency of 75–80% at the time of irradiation. After attachment, incubate the cells with fresh serum-containing DMEM supplemented with 1X hypericin solution. The concentration of hypericin and the duration of incubation are determined and optimized for every cell line. Usually a range between 0.05 and 1 μM hypericin is used in most experiments.
2. Incubate the plates protected from light exposure at 37°C.
3. If pharmacological compounds (e.g., inhibitors) are used, add 1 h prior to irradiation (*see* **Note 1**).
4. Collect the medium in Falcon tubes and cover the cells in pre-warmed PBS for the duration of the irradiation period.
5. Place the cell culture plates on a plastic diffuser sheet above a set of seven L18W30 fluorescent lamps (Osram). The fluence rate of the lamps is 4.5 mW/cm^2 as measured with an IL 1,400 radiometer (International Light, Newburyport, MA). The fluence or light dose (J/cm^2) is calculated by multiplying the fluence rate with the time of irradiation. Usually a light dose between 1.9 and 2.7 J/cm^2 is used.
6. Replace PBS with the original medium and put the plates back in the incubator at 37°C protected from light until further analysis.

3.2. Preparation of Protein Lysates

1. At the required time points, remove the plates from the incubator and put them on ice. Collect the medium in Falcon tubes. Wash the cells once with 5 ml pre-chilled PBS.
2. Scrape off the cells from the plate in 5 ml pre-chilled PBS on ice and collect the suspension in a new Falcon tube. Centrifuge both suspensions (floating cells and attached cells) at 500×*g* for 5 min.
3. Aspirate the supernatants and resuspend the pellets combined in HEPES lysis buffer in a total volume adapted to the size of the pellet (50–100 μl). Transfer the samples to pre-chilled eppendorfs.
4. Perform lysis on ice for 15 min followed by centrifugation at 16,000×*g* for 15 min at 4°C to pellet cell debris, nuclei, and membranous components. Remove the supernatant carefully (without disturbing the pellet) and transfer it to new pre-chilled eppendorfs. Immediately store at –20°C.

3.3. Gel Electrophoresis and Western Blotting

1. Determine protein concentration and prepare samples to obtain equal protein loading (e.g., 20–40 μg, *see* **Note 2**). Add 1:6 volume of 6X loading buffer to the samples. Spin down and boil the samples for 5 min in a heating block at 100°C.
2. Load samples on a precast Criterion^{TM} XT gel and separate samples by SDS-PAGE (Criterion^{TM} Cell; Bio-Rad

Laboratories, Hercules, CA, USA). 4–12% Bis–Tris gels are chosen to allow good separation of proteins ranging between 100 and 10 kDa. To separate higher MW proteins in the range of 75–250 kDa, 3–8% Tris-Acetate gels are used. Stop gel electrophoresis just before the bromophenol blue-stained front runs off the gel.

3. Enclose the gel in a blotting cassette (Criterion^{TM} Blotter; Bio-Rad Laboratories, Hercules, CA, USA) and transfer proteins to a Protran 2-μm pored nitrocellulose paper (Perkin-Elmer, Boston, MA, USA).
4. Block the membrane for 1 h in a 5% non-fat milk powder solution: For chemiluminescent detection (ECL) the milk powder is dissolved in TBS-Tween. For infrared (IR) fluorescence detection with the Odyssey near-IR detection (LiCor Biosciences, Lincoln, NE, USA) system, the milk powder is dissolved in TBS without Tween (*see* **Note 3**).
5. Incubate the membrane with the appropriate primary antibody diluted in blocking buffer, ON at 4°C with gentle shaking.
6. Wash the membrane three times for 10 min in an excess amount of TBS-Tween.
7. Incubate the membrane with a secondary antibody in blocking buffer for 2 h at 4°C with gentle shaking: For ECL – 1:2,000 dilution of the HRP-labeled secondary antibody (ab), for Odyssey – 1:5,000 dilution of the IR-labeled secondary ab, and incubate and wash the membranes in dark conditions.
8. Wash the membrane three times for 10 min in an excess amount of TBS-Tween.
9. For ECL: Cover the membrane with the ECL reagent mixture (ECL Western blotting substrate, Pierce, Rockford, IL, USA) for 1 min and place it between two transparent plastic sheets. Wipe out excess amounts of reagents and expose the membrane to a light-sensitive film Cronex5 medical X-ray film (AGFA-Gevaert, Mortsel, Belgium) in a light-safe cassette. The duration of the exposure of the membrane to the light-sensitive film varies, depending on the primary antibody used. For Odyssey: the membranes are scanned on the Odyssey InfraRed Imager.

3.4. Assessment of Apoptosis in PDT-Treated cells

In this section we will detail protocols to detect and quantify apoptotic cell death, based on the determination of DNA fragmentation, assays of mitochondrial outer and inner membrane permeabilization and release of mitochondrial intermembrane proteins and caspase activity following hypericin–PDT. Additionally we detail a protocol for the discrimination of cell death morphology by TEM analysis.

3.4.1. Determination of Caspase Activity

At the biochemical level apoptosis entails the activation of caspases, a highly conserved family of cysteine-dependent aspartate-specific proteases. All caspases share an active-site cysteine residue and the specific requirement for a four-amino acid recognition motif that terminates in aspartic acid for cleavage. Caspases are synthesized as proenzymes or zymogens, consisting of a prodomain of variable length, followed by p20 and p10 subunits containing residues critical for the recognition of the substrate and the catalytic activity. Caspases are activated in response to an apoptotic signal by proximity-induced dimerization at a multimeric protein complex (initiator caspases), which is followed by autocatalytic processing, or by limited proteolysis by an upstream caspase (effector caspases) (11). In both cases the end result is the separation of the prodomain from the p20 and p10 subunits generating an active heterotetramer. Proteolytic activation of caspases can be detected by the appearance of the p20 and p10 fragments and the concomitant decrease in the inactive zymogen by Western blotting. It is generally accepted that once activated, the effector caspases are responsible for most of the stereotypic morphological and biochemical changes observed during apoptosis by cleaving a restricted subset of vital substrates like the nuclear protein poly(ADP-ribose)polymerase (PARP). Activation of caspases does not occur during necrotic or autophagic cell death. Thus, detection of caspase activity during the cell death process and its sensitivity to inhibition by inhibitors of caspases can be used to discriminate between apoptosis (caspase-mediated) and other cell death modalities. Measurement of caspase activity requires the use of synthetic substrates for caspases. These substrates are usually tetrapeptides with aspartate at the position P1, within the primary structure "XXXD," conjugated with a fluorogenic AMC (7-amino-4-methylcoumarin) or AFC (7-amino-4-trifluoromethylcoumarin) group. Hydrolysis of the substrate by active caspase results in the release of free AMC or AFC groups which are fluorescent and can be measured in a fluorometer.

3.4.1.1. Determination of Caspase Processing and Substrate Proteolysis by Western Blotting

Western blot procedures are performed according to the protocols detailed in **Section 3.3**. The caspase 3 and PARP antibodies are both diluted 1:5,000 in blocking buffer. A representation of caspase 3 processing and PARP cleavage after hypericin–PDT treatment is displayed in **Fig. 2.1**.

3.4.1.2. Caspase Activity Assay

1. Lysates for this caspase activity assay are made according to protocol in **Section 3.2** with a specific lysis buffer detailed as the "assay buffer" in **Section 2.4.1**. In this assay buffer, the proteasome inhibitor cocktail is modified not to compromise caspase activity.

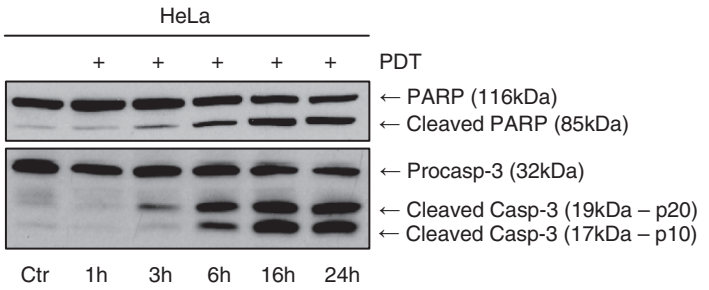

Fig. 2.1. PDT-induced caspase-3 activation and substrate cleavage. At the indicated time points after irradiation (controls are incubated with hypericin but not irradiated) total protein lysates were made and processed for Western blotting according to protocols in **Sections 3.3** and **3.4.1**. Chemiluminescent detection reveals the increased accumulation of the active p10 and p20 fragments of caspase-3, which parallels the proteolytic processing of its downstream substrate PARP.

2. On a 96-well plate, incubate lysates containing 50 μg of proteins with 50 μM of the fluorescent substrate Ac-DEVD-AMC (for caspase 3 and 7) in a total volume of 250 μl assay buffer at 37°C for 30 min (*see* **Note 4**). A condition carrying only assay buffer with the fluorescent substrate is used as a negative control.
3. Measure kinetics of DEVD-AMC cleavage for 40 min with a 2 min interval between the readings, with fluorospectrometer pre-warmed to 37°C. For AMC the excitation is at 360 nm and the emission is measured at 460 nm.
4. Normalize the raw data by subtracting the value of the negative control from the raw data per time point. Plot the normalized data vs time. The best fitting curve is calculated and the slope of the curve can be used to calculate the amount of fluorescence produced per minute.

3.4.2. Determination of DNA Fragmentation by Sytox Green Staining

DNA fragmentation is a hallmark of apoptosis. Activation of various apoptotic nucleases during cell death results in the formation of high molecular weight (>50 kbp) and nucleosome-sized (200 bp) DNA fragments. Based on this apoptotic parameter, different techniques, which include separation of DNA ladders by agarose gel electrophoresis, fluorescence imaging of nuclear fragmentation with 4′,6-diamidino-2-phenylindole dihydrochloride (DAPI), Hoechst, or propidium iodide (PI), and terminal deoxynucleotidyl transferase-mediated dUTP nick end labeling (TUNEL), have been developed (*see* **Note 6**). A particularly useful technique is the determination of the cell's "hypoploid" or sub-G1 DNA content by flow cytometry. This technique provides information on the distribution of the cell population within the major phases of the cell cycle, while estimating the frequency

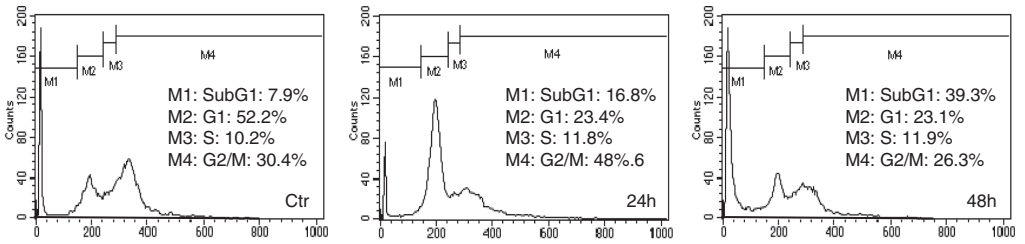

Fig. 2.2. PDT-induced DNA fragmentation in HeLa cells. At 24 and 48 h after hypericin–PDT treatment, the cells were harvested and stained with Sytox Green according to protocol in **Section 3.4.2** and compared with control cells (hyp-incubated but not irradiated). DNA fragmentation in the population of cells increases over time (indicated by the SubG1 fraction) as a late event in the degradation phase of apoptosis.

of apoptotic cells with a hypoploid DNA amount. Typically, a healthy population of nonsynchronized cells will exhibit a biphasic peak of $2n$ (G1) and $4n$ (G2) cells. Upon apoptosis induction a fraction of cells showing a lower DNA fluorescent pattern, as the result of DNA fragmentation, appears as a "sub-G1 peak." For hypericin–PDT, we use Sytox Green, a green fluorescent DNA dye, as detailed below (**Fig. 2.2**).

1. After irradiation of the cells on 10-cm culture dishes, collect the medium in a Falcon tube and wash the cells once with 5 ml PBS pre-warmed at 37°C.
2. Trypsinize cells with 1 ml of pre-warmed (37°C) trypsin solution. Since the integrity of the cells has to be maintained to the highest possible extent this procedure is preferred over scraping the cells of the plate.
3. Stop trypsinization by adding 1 ml serum-containing DMEM and collect the cells in the Falcon tube.
4. Centrifuge the cells for 5 min at 100×*g*. Aspirate the supernatant and resuspend the pellet in 300 µl PBS and transfer it into eppendorfs.
5. Add 1.5 ml of ice-cold 70% ethanol (EtOH) and allow fixation overnight (ON) at –20°C.
6. Centrifuge the cells for 10 min at 2,500×*g* and aspirate the EtOH carefully. Wash once with 1.5 ml PBS and centrifuge for 10 min at 2,500×*g*.
7. Aspirate the supernatant and resuspend the pellet in 0.5 ml PBS. Add 1 ml DNA extraction buffer. Incubate 5 min at room temperature (RT).
8. Centrifuge for 10 min at 2,500×*g* and aspirate off the supernatant. Resuspend the pellet in 0.5 ml DNA staining solution (*see* **Note 7**). Incubate for 30 min at RT.
9. Perform flow cytometric analysis.

3.4.3. Assessment of Mitochondrial Outer and Inner Membrane Permeabilization

Detection of outer membrane (OM) permeabilization relies mainly on the analysis of the subcellular redistribution of proteins that are usually retained within the intermembrane space (IMS) (i.e., the space formed between the inner and outer membrane of the mitochondria) by the OM, following PDT. This is usually performed by immunoblot detection of such proteins, which include primarily cytochrome *c*, but can also be extended to other proapoptotic molecules trapped in the IMS, such as AIF, EndoG, Smac/DIABLO, and Omi/HtrA2 (12), upon isolation of different subcellular fractions (e.g., cytosol and mitochondria). Usually this approach requires that a mild detergent permeabilizing the plasma membrane while leaving intact the mitochondrial membrane, such as digitonin, is used to avoid that IMS proteins' leak out during organelle and subcellular preparation. Since IMS proteins are released with variable kinetics, depending on the type of photosensitizer and the cells used (4), it is advisable to perform kinetic studies and monitor the subcellular localization of several IMS proteins rather than of a single one. Assessment of IM permeability, which often occurs during cell death, relies on the use of IM-permeant lipophilic cations that accumulate in the mitochondrial matrix. Since under normal circumstances, the $\Delta\psi_m$ ranges from 120 to 180 mV (the intramitochondrial side being electronegative), these lipophilic cations concentrate in the mitochondrial matrix driven by the $\Delta\psi_m$ following the Nernst equation. These fluorochromes include, but are not limited to, rhodamine 123 (Rh 123), tetramethyl rhodamine ethyl and methyl esters (TMRE and TMRM, respectively), chloromethyl-*X*-rosamine (CMXRos, also known as MitoTracker Red), 5,5′,6,6′-tetrachloro-1,1′,3,3′-tetraethylbenzimidazolcarbocyanine iodide (JC-1), and 3,3′-dihexyloxacarbocyanine iodide (DiOC6(3)). The choice of the fluorochrome is dictated by their spectral properties, since this analysis is performed in living cells loaded with the fluorescent dye. For hypericin, which has a maximal absorption spectrum at 595 nm, we load the cells with the carbocyanine DiOC6(3) (max. abs. 484 nm) followed by quantification of the cell population with high (untreated) or low DiOC6(3) staining (PDT treated) by flow cytometric analysis (**Fig. 2.3**).

Additionally, two-color immunofluorescence staining (*see* **Section 3.4.3.3**) can be employed to visualize the co-localization of IMS proteins, such as cytochrome *c* or AIF, with specific mitochondrial markers (e.g., cytochrome *c* oxidase subunit IV) or using organelle-specific fluorescent markers (e.g., MitoTracker® Red CMXRos). Often nuclear counterstaining and/or the use of antibodies specific for active caspases are used to provide supplementary information about the apoptotic cascade induced by PDT.

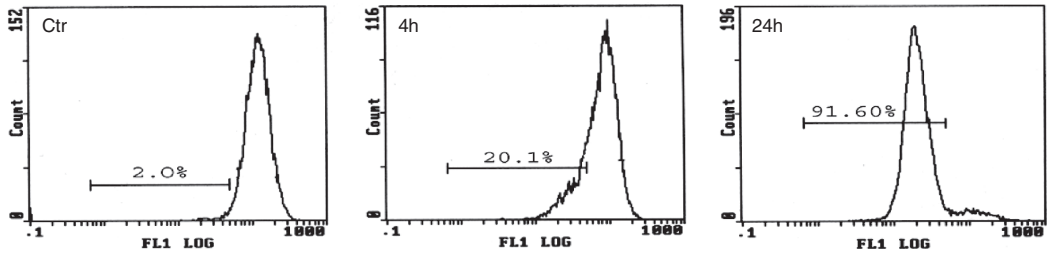

Fig. 2.3. PDT-induced mitochondrial membrane depolarization in HeLa cells. At 4 and 24 h after hypericin–PDT treatment, the cells were harvested and stained with DiOC6(3) according to protocol in **Section 3.4.3** and compared with the control cells (hyp-incubated but not irradiated). The gate indicates the increasing fraction of cells with depolarized mitochondria over time. The mitochondrial depolarization is an early event in the induction of apoptosis and clearly precedes the DNA fragmentation depicted in Fig. 2.2.

3.4.3.1. Subcellular Fractionation with Digitonin

1. At the required time points after PDT, remove the plates from the incubator and place them on ice. Collect the medium in a Falcon tube and spin down detached cells at 100×*g*. Meanwhile, wash the cells in the culture plates once with 5 ml ice-cold PBS, aspirate the PBS, and add 5 ml fresh ice-cold PBS.
2. Resuspend cell pellet in ice-cold PBS. Scrape off the cells from the plate in the PBS on ice and collect the suspension in the Falcon with resuspended cell solution (in this way both attached and floating cells are collected). Centrifuge the suspension mildly at 100×*g* for 5 min to avoid physical rupture of the membranes and organelles.
3. Aspirate the supernatant and resuspend the pellet shortly in 150 µl of digitonin buffer. Collect the suspension in pre-chilled eppendorfs and immediately centrifuge for 20 min at 16,000×*g* at 4°C. Only a short incubation in the soft detergent digitonin will break the plasma membrane without compromising the integrity of the organelle membranes. A fast transfer of the resuspended pellet to the eppendorfs and the subsequent centrifugation are therefore essential steps in this experimental approach (*see* **Note 8**).
4. Transfer the supernatant (supernatant A), without disturbing the pellet (pellet A) to a pre-chilled eppendorf. Supernatant A contains all soluble proteins, including the released mitochondrial intermembrane proteins. Pellet A contains the intact cells, the intact organelles, and the plasma membrane.
5. Resuspend the pellet A in 150 µl of HEPES lysis buffer and incubate on ice for 15 min. Centrifuge the lysates at 16,000×*g* for 15 min at 4°C.
6. Transfer the supernatant (supernatant B) without disturbing the pellet (pellet B) to a new pre-chilled eppendorf. This

supernatant contains proteins recovered from the organelle fraction and plasma membrane.

7. Measure protein concentration of supernatant A and B and perform Western blotting for cytochrome *c*, using a 1:1,000 dilution of the anti-cytochrome *c* antibody.
8. Check the purity of the soluble and mitochondrial fractions by the specific immunodetection of cytoplasmic, like actin (anti-actin antibody is diluted 1:50,000) or mitochondrial proteins, like cytochrome oxidase subunit IV (anti-cytochrome *c* oxidase subunit IV is diluted 1:1,000), in the respective subcellular fractions.

3.4.3.2. DiOC6(3) Staining for Mitochondrial Inner Membrane Depolarization

1. After treatment, wash the cells once with 5 ml of pre-heated PBS at 37°C and trypsinize them with 1 ml pre-warmed trypsin solution for 5 min.
2. Stop trypsinization by adding 1 ml serum-containing DMEM and collect the cells in a Falcon tube.
3. Centrifuge the cells (100×*g* for 5 min) and resuspend the pellet carefully in serum-containing DMEM with 40 nM of DiOC6(3) (*see* **Note 9**) and further incubate for 30 min at 37°C in dark conditions.
4. Centrifuge the cells (100×*g* for 5 min), wash the pellet once with pre-chilled PBS, and keep it on ice until analysis.
5. For large cell populations the analysis of $\Delta\psi_m$ is performed on a flow cytometer. The loss of transmembrane potential in treated cells is measured as a decrease in DiOC6(3) green fluorescence (*see* **Note 10**).

3.4.3.3. Immunocytochemistry

1. For immunocytochemistry the cells are plated and treated on two-chamber slides.
2. After PDT, and 30 min prior to the staining procedure, add 50 nM of MitoTracker® Red CMXRos (Molecular Probes, Invitrogen, Carlsbad, CA, USA) to the culture medium and incubate at 37°C.
3. Wash the slides carefully with 1 ml of ice-cold PBS.
4. Fix the cells with 1 ml 4% paraformaldehyde diluted in PBS pH 7.4 for 20 min. Aspirate the paraformaldehyde and wash three times for 3 min with 1 ml PBS with gentle shaking.
5. Permeabilize the cells with 1 ml of 0.1% (v/v) Triton X-100 solution in PBS for 10 min. Aspirate the Triton solution and wash three times for 3 min with 1 ml PBS with gentle shaking.
6. Incubate the slides twice with 1 ml 0.1 M glycine solution for 10 min. Glycine will neutralize the ionic charges on

proteins and will prevent unspecific binding of the primary and secondary antibodies.

7. Wash once with 1 ml of PBS with gentle shaking.
8. Block the slides for 20 min with a 1% (ultrapure grade) BSA solution in PBS complemented with 10% serum derived from the host species in which the secondary antibody was raised. This will suppress non-specific binding of IgG during the staining.
9. Blot the excess serum and incubate the chambers with 400 μl of the primary anti-cytochrome *c* antibody, diluted 1:500 in 1% BSA–PBS, supplemented with 10% serum for 1 h.
10. After incubation, aspirate the antibody solution and wash four times for 3 min with 1 ml PBS with gentle shaking.
11. Incubate with 400 μl of the Alexa488-labeled secondary antibody diluted 1:1,000 in 1% BSA–PBS, supplemented with 10% serum for 1 h. After the staining, aspirate the antibody solution and wash four times for 3 min with 1 ml PBS with gentle shaking.
12. Blot all excess liquids and mount the slides with a drop of Prolong Gold antifade reagent containing DAPI (Invitrogen, Carlsbad, CA, USA), cover the slides with a cover glass, and allow curing for 24 h at 4°C. The DAPI in the mounting medium will provide a blue fluorescent counterstaining of the nuclei.
13. Image samples on a fluorescent microscope.

3.5. Transmission Electron Microscopy (TEM) for the Study of Cell Death

Although TEM is time consuming and requires expensive equipment, this technique has been considered a "golden standard" in cell death research. It offers high-resolving power (0.1–0.4 nm), thereby providing much more detailed information about cell morphology as compared to conventional light microscopy. Two of the earliest ultrastructural changes detectable in apoptosis via TEM are formation of uniformly dense masses of chromatin distributed against the nuclear envelope (**Fig. 2.4**) and persistence of a nucleolar structure until the very late stages (13, 14). Apoptotic cells are further characterized by the loss of specialized surface structures, such as microvilli and cell–cell contacts, condensation of cytoplasm, and formation of membrane-bound apoptotic bodies of different sizes containing well preserved but compacted cytoplasm organelles and/or nuclear fragments (**Fig. 2.4**) (13, 15). Necrosis is morphologically distinct from apoptosis and is characterized by a general swelling of the cell (oncosis) and cytoplasmic organelles and rapid loss of plasma membrane integrity (16). The nuclear morphology remains relatively unchanged until later stages, when chromatin condenses into small irregular pieces (**Fig. 2.4**).

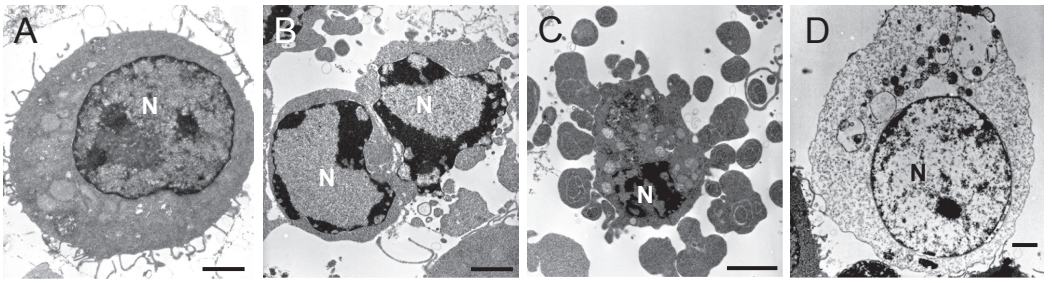

Fig. 2.4. Analysis of cell morphology of apoptotic and necrotic cells by transmission electron microscopy. J774A.1 macrophages were treated with 300 μM spermine NONOate for 3 h. (**a**) Untreated cell showing microvilli protruding from the entire surface, a smoothly outlined nucleus with chromatin in the form of heterochromatin and well-preserved cytoplasmic organelles. (**b**) Two apoptotic cells with sharply delineated masses of condensed chromatin. (**c**) Apoptotic cell with convolution of the cellular surface and formation of apoptotic bodies. (**d**) Necrotic cell containing clumps of chromatin with ill-defined edges, swollen mitochondria, and electron lucent cytosol. Scale bar = 2 μm. N indicates nucleus.

These instructions assume the use of suspension cells (*see* **Note 11**).

1. Centrifuge cells (1–2 × 10^6 cells) at 100×*g* for 5 min.
2. Remove the supernatant and add 4 ml 0.1 M sodium cacodylate-buffered (pH 7.4) 2.5% glutaraldehyde solution to the pellet without resuspending the cells. Allow fixation for 2 h at 4°C.
3. Remove fixative and rinse cell pellet (3 × 10 min) with 5 ml 0.1 M sodium cacodylate-buffered (pH 7.4) 7.5% saccharose without resuspending the cells (*see* **Note 12**).
4. Add 3–4 ml 1% osmium tetroxide (OsO_4) in 0.033 M veronal acetate buffer containing 4% saccharose. Allow postfixation for 2 h at 4°C.
5. Remove OsO_4 solution and rinse cell pellet (3 × 10 min) with 5 ml 0.05 M veronal acetate buffer containing 6% saccharose.
6. Dehydrate cell pellet in an ethanol gradient as follows: 70% ethanol (15 min), 90% ethanol (15 min), 96% ethanol (15 min), and 100% ethanol (5 × 20 min).
7. Treat cell pellet with the following ethanol/Durcupan ACM (Fluka, Bornem, Belgium) mixtures at room temperature: Ethanol/Durcupan ACM (3:1) (1 h), ethanol/Durcupan ACM (1:1) (1 h), and ethanol/Durcupan ACM (1:3) (1 h).
8. Incubate cell pellet in Durcupan ACM1 containing 10 ml Durcupan component A (embedding substance), 10 ml Durcupan component B (hardener), and 0.15 ml Durcupan component D (plasticizer) at 40°C (2 × 90 min).
9. Incubate cell pellet in Durcupan ACM2 containing 10 ml Durcupan component A, 10 ml Durcupan component B,

0.35 ml Durcupan component C, and 0.15 ml Durcupan component D at 40°C (90 min).

10. Transfer cell pellet into a gelatin capsule, cover with Durcupan ACM2, and allow polymerization at 60°C for 3 days.
11. Cut ultrathin sections (±50 nm thick) with an ultramicrotome using a diamond knife (Element Six, Berkshire, UK).
12. Capture and air-dry sections on 200-mesh copper grids (Canemco, Quebec, Canada).
13. Stain sections with 2% uranyl acetate for 15 min in the dark. Rinse sections with ultrapure water.
14. Stain sections with Reynolds solution pH 12.4 for 10 min. Rinse sections with 0.05 M NaOH Titrisol and CO_2-free ultrapure water (*see* **Note 13**).
15. View samples with a TEM at an accelerating voltage of 80 kV.

3.6. Methods to Monitor Autophagy

At the onset of the process of autophagy, the cytosolic protein LC3 (LC3-I) is lipidated to LC3-phosphatidylethanolamine (LC3-II) and targeted to the autophagosomal membranes. Although the molecular weight of the cytosolic LC3-I is estimated to be 18 kDa and the addition of the PE tail significantly increases its molecular weight, the hydrophobic nature of PE causes a faster migration of the lipoprotein LC3-II during SDS gel electrophoresis resulting in an apparent molecular weight of only 16 kDa. The conversion of LC3-I to LC3-II, which is thought to correlate well with the amount of autophagosomes present in a cellular system, by Western blotting has become an accepted biochemical marker of autophagy (17) as shown in **Fig. 2.5a**. Another well-explored method requires the ectopic expression of a GFP-LC3 chimeric protein followed by fluorescence imaging. Under normal conditions, GFP-LC3 is cytosolic and will display a diffuse pattern of green fluorescence, while upon autophagy stimulation the association of LC3-II to the autophagosomes will increase the concentration of GFP at the autophagosomal membranes, resulting in the visualization of a typical punctuated pattern (**Fig. 2.5b**). Counting the amount of GFP-punctuae per cell provides an excellent method for the quantification of autophagosomes after PDT. Based on the same principle LC3 relocalization can be visualized by immunostaining for the endogenous LC3. However, due to the transient nature of autophagosomes (half-life is 20–30 min) and the basal levels of autophagy as a homeostatic process, an increased LC3 conversion seen on Western blot might indicate either the stimulation of autophagy (increased ON rate) or the inhibition of the degradation of autophagosomes (decreased OFF rate). Only the evaluation of "autophagic flux," the degradation of autophagosomes, and their cargo can distinguish the two events. Pharmacological inhibitors

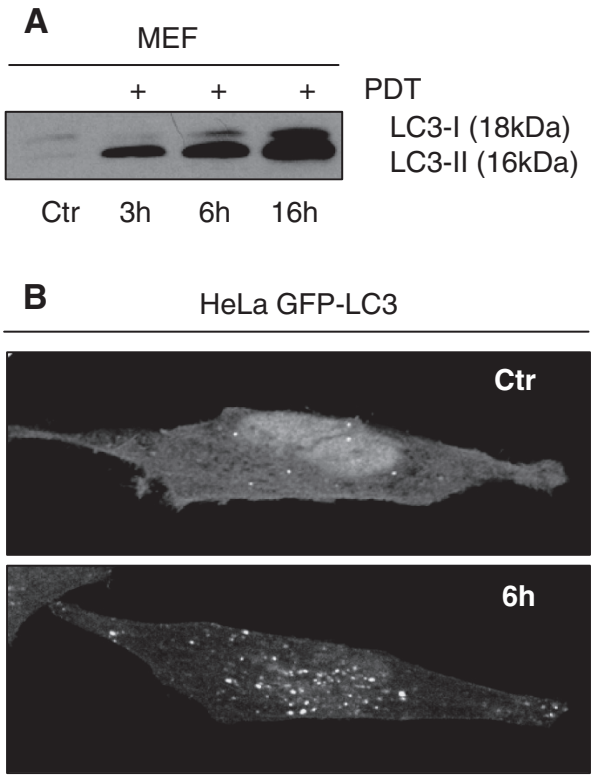

Fig. 2.5. Formation of autophagosomes after hyp-PDT. (**a**) At the indicated time points after irradiation (controls are incubated with hypericin but not irradiated) total protein lysates were made from MEFs and processed for Western blotting according to protocols in **Sections 3.3** and **3.6.1**. Chemiluminescent detection reveals both an induction of LC3-I and a simultaneous conversion to LC3-II, suggesting the formation of autophagosomes after PDT. (**b**) Seventy-two hours before PDT treatment, HeLa cells were transiently transfected with GFP-LC3, according to protocol in **Section 3.6.2**. Six hours after treatment, the cells were visualized on a confocal microscope. The punctuated pattern apparent at the 6 h time point indicates the formation of autophagosomes after hyp-PDT, as also suggested by the Western blot in the *upper panel* (**a**).

of the lysosomal–autophagosomal fusion, such as BafilomycinA1 (BafA1), prevent the formation of autolysosomes and result in the inhibition of LC3-II degradation and autophagic flux. Thus, only if the ON rate of autophagy has been stimulated by PDT, this will result in a superimposed detection of LC3-II caused by the accumulation of autophagosomes. If after co-treatment with BafA1 no increase in LC3-II detection is noticed, one can assume that PDT interferes with the autophagosome–lysosome fusion, limiting the OFF rate. Additionally, in cells transfected with GFP-LC3, GFP is readily separated from LC3-II in the inner membrane during the degradation phase but is very resistant to mammalian hydrolysis. This allows for the monitoring of the accumulation of "free GFP" on Western blot as an accumulating degradation product of autophagy and therefore an event truly representative

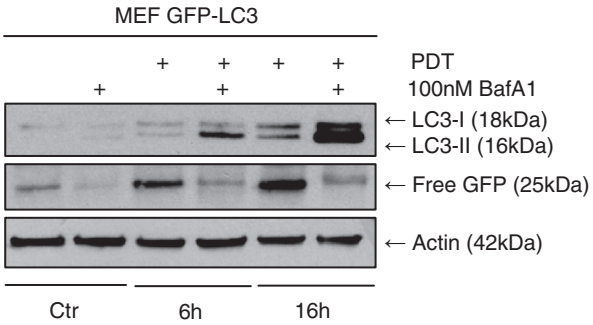

Fig. 2.6. Stimulation of autophagic flux after hyp-PDT. MEFs stably expressing GFP-LC3 were PDT treated and at the indicated time points full protein lysates were made for Western blot application as described in **Sections 3.3** and **3.6.3**. Where indicated 100 nM BafA1 was added to the incubation medium 1 h prior to irradiation. The detection of increasing amounts of "free GFP" indicates the stimulation of autophagic flux which can be inhibited with BafA1. The superimposed detection of LC3-II in the case of BafA1 co-treatment further substantiates the activation of autophagic flux (increased ON rate) after hyp-PDT. Control cells were incubated with hypericin but not irradiated.

for autophagic flux. BafA1 pretreatment inhibits autophagic flux and diminishes the release of "free GFP" (**Fig. 2.6**). Apart from the identification of apoptotic and necrotic cells, TEM analysis remains one of the most sensitive methods to detect the accumulation of autophagic compartments in mammalian cells (**Fig. 2.7**). Autophagosomes are by definition membrane-bound structures that contain cytoplasm (i.e., cytosol and possibly organelles). Structures that do not fulfill this criterion should not be classified as autophagosomes or autophagic vacuoles. Because of the subjective nature of this morphological analysis (*see* **Note 14**), TEM as a method to monitor autophagosomes has to be complemented with other techniques described in this chapter.

3.6.1. LC3 Detection on Western Blot

Total protein lysates are made according to the protocol in **Section 3.2** (*see* **Note 15**). Detection of LC3 on Western blot is carried out according to the protocols described in **Section 3.3**. The LC3 antibody is diluted 1:800 in blocking buffer (*see* **Notes 16** and **17**).

3.6.2. Visualization of Autophagosomes by Overexpressing GFP-LC3 (see Note 18)

1. On day 0, seed HeLa cells at a density of 5×10^5 cells per 10-cm plate. On day 1 transfect cells with GFP-LC3 using FuGENE® HD (Roche Applied Science, Indianapolis, IN, USA):
   a. Replace the medium of the cells with 5 ml antibiotics-free DMEM supplemented with 10% FBS.
   b. Incubate 10 μg vector DNA carrying GFP-LC3 with 15 μl FugeneHD in a total volume of 500 μl DMEM for 15 min at RT.

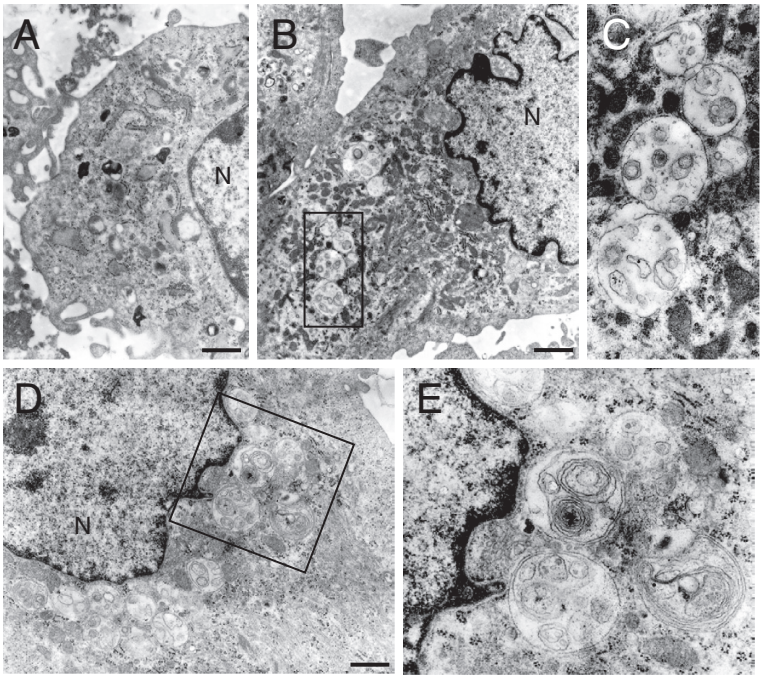

Fig. 2.7. Analysis of cell morphology of autophagic cells by transmission electron microscopy. C2C12 cells were subjected to amino acid deprivation for 12 h. (**a**) Untreated cell showing a normal cell morphology. (**b**–**e**) Starved cells with numerous autophagic vesicles in the cytosol. (**c**) The *boxed area* in *panels* **b** and **d** is shown at higher magnification in *panels* **c** and **e**, respectively. Scale bar = 1 μm. N indicates nucleus.

c. Add this solution to the cells medium and incubate the plates for 24 h at 37°C.

2. On day 2, replate the transfected cells to a density of 3×10^5 cells per 6-cm plate or 5×10^4 cells per chamber on a chamber slide. This ensures equal expression (*see* **Note 19**) of GFP-LC3 in all conditions tested.
3. Incubate plates for at least 48 h, or up to 72 h, before analysis on the microscope (*see* **Note 20**).

3.6.3. Autophagic Flux

1. One hour prior to irradiation, 100 nm of BafA1 is added to the medium (*see* **Note 21**).
2. The following steps are carried out according to the protocol described in **Section 3.6.1** for LC3 detection or combined with **Section 3.6.2** if the cells are transfected with GFP-LC3.

3.6.4. Detection of Autophagosomes by TEM

See **Section 3.5**.

3.7. Methods to Monitor MAPK and Akt-mTOR-Signaling Cascades

Signaling pathways governed by the Ser/Thr protein kinases MAPKs and Akt (also known as protein kinase B, PKB) regulate both apoptosis and autophagy. In mammalian cells the three major MAPK family members include the extracellular signal-regulated kinases (ERK 1 and 2), which are typically stimulated in response to growth and differentiation signals, the c-Jun amino-terminal kinases (JNK 1, 2, and 3), and the p38 MAPKs (p38 $\alpha/\beta/\gamma$ and δ), which are activated by a diverse array of stress signals (18). Common for all family members of the MAPKs is the activation by an upstream MAP2K through phosphorylation on a conserverd Thr-X-Tyr motif. Activation of the different MAPKs results in either pro- or anti-apoptotic effects depending on the cellular background and the type of stress.

Cytosolic Akt is recruited to the plasma membrane following the generation of phosphatidylinositol (3,4,5)-trisphosphate (PIP3) by the growth factor-mediated activation of class I PI3 kinase (PI3K), where it becomes phosphorylated on Thr308 and Ser473 by 3-phosphoinositide-dependent kinase-1 (PDK1) and by PDK2, respectively, resulting in its activation (19). Akt activation not only leads to the suppression of apoptosis, a well-studied functional outcome of this pleiotropic pathway, but also of autophagy through the activation of the mammalian target of rapamycin (mTOR). mTOR is a Ser/Thr kinase which, upon activation, leads to inhibition of autophagy while favoring anabolic pathways, such as mRNA translation via the activation of its direct downstream target p70-S6 kinase (20). Whereas the role of MAPKs in PDT has been abundantly scrutinized (2, 21), the role of the Akt-mTOR pathway is still largely unexplored.

Since the activation mechanism of these kinases and often of their downstream kinase substrates entails the phosphorylation of specific residues, a convenient method to monitor the activation status of these signaling cascades after PDT relies on Western blot analysis with antibodies that specifically recognize either the phosphorylated/active or non-phosphorylated/inactive forms of these kinases. If possible, detection of the activation status is performed preferentially by infrared (IR) fluorescence detection with the Odyssey® Imaging System (LiCor Biosciences, Lincoln, NE, USA). This detection method offers several advantages over the classical chemiluminescent method. The use of infrared wavelengths dramatically reduces autofluorescence and light scatter conferring a clean background, high signal-to-noise ratio, and sensitivity. The presence of two different infrared channels allows for probing two separate targets in the same experiment simultaneously (multiplex detection), which makes normalization easy and eliminates errors introduced by stripping and reprobing or by comparison of separate blots. In this way, both

the phosphorylated form and the total amount of a given protein (kinase) can be detected at the same time (two-color Western), with the only requirement being the availability of phospho- and total protein-directed antibodies from two different sources (i.e., rabbit and mouse). Additionally, the wide linear dynamic range and accompanying software makes fast and accurate quantification possible. For example, the activation status of mTOR can be monitored indirectly by assessing the phosphorylation status of p70-S6 kinase and its substrate the S6 ribosomal protein. Additionally, kinase immunoprecipitation followed by in vitro kinase assays using specific model substrates has been employed in previous studies (8).

In general, kinetic experiments in PDT exposed cells should be initially performed due to the dynamic regulation of these kinases by (de-)phosphorylation events.

Preparation of lysates and Western blot procedures are performed according to the protocols detailed in **Sections 3.2** and **3.3**, respectively (*see* **Note 22**).

3.7.1. ECL as Detection Method

1. Incubate the membrane with phospho-specific primary antibody diluted in 5% BSA in TBS-T, ON at 4°C with gentle shaking (**Fig. 2.8a**).
2. Proceed for ECL detection of phosphorylated protein as described in Step 9 of protocol in **Section 3.3**.
3. After detection, incubate the membrane in 50 ml stripping buffer for 15 min at 65°C.
4. Wash the membrane several times with fresh TBS-T to remove all traces of β-mercaptoethanol.
5. Incubate the membrane in blocking buffer for 1 h at RT with gentle shaking.
6. Incubate the membrane with the primary antibody for the detection of the total protein diluted in 5% BSA in TBS-T, ON at 4°C with gentle shaking.
7. Proceed for ECL detection of total protein as described in Step 9 of protocol in **Section 3.3**.

3.7.2. Odyssey as Detection Method

1. Because Tween emits IR fluorescence that is detected in the 700 nm channel of the Odyssey, block the membranes in 5% BSA dissolved in TBS without Tween for 1 h at RT with gentle shaking (**Fig. 2.8b**).
2. Incubate the membrane with both phospho-specific and total protein primary antibodies diluted in 5% BSA in TBS-T, ON at 4°C with gentle shaking (*see* **Note 23**).
3. Wash the membrane three times for 15 min in an excess amount of TBS-T.

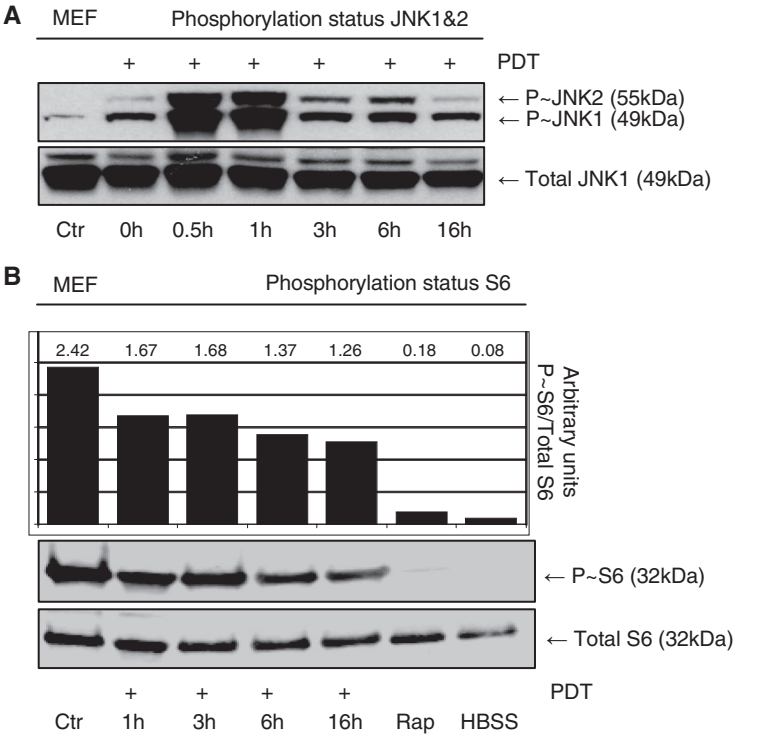

Fig. 2.8. Monitoring the activation status of phosphoproteins. At the indicated time points after PDT, full protein lysates were made for Western blot detection according to the protocols in **Sections 3.2** and **3.3**. Determination of phosphorylation status was performed according to protocol in **Section 3.7.1**. (**a**) *ECL as a detection method* – After the detection of phospho-JNK1 and 2, the membrane was stripped, blocked, and reprobed for the detection of total JNK1. (**b**) *Odyssey as detection method* – Phospho-ribosomal protein S6 (P-S6) and total ribosomal protein S6 (S6) were simultaneously monitored on the Odyssey IR Imager. The graph represents the quantification of the Western blot and is expressed as the level phospho-S6 normalized to the total amount for each time point. Where indicated, samples were treated with 100 nM rapamycin (Rap) or a 2 h starvation in Hank's balanced salt solution (HBSS), two known inducers of autophagy. In all experiments, control cells were incubated with hypericin but not irradiated.

4. Incubate the membrane with both IR-labeled secondary antibodies, diluted 1:5,000 in 5% BSA dissolved in TBS-T for 1 h at RT with gentle shaking.
5. Wash the membrane in subdued light conditions two times for 15 min in an excess amount of TBS-T and once for 15 min with TBS.
6. Scan the membranes on the Odyssey IR Imager for simultaneous detection of phospho- and total protein levels.
7. Use Odyssey software to quantify phospho- and total protein levels and plot the phospho-/total protein ratio.

4. Notes

1. Preliminary experiments with appropriate activity assays should be carried out to define the optimal pre-incubation time for every compound. Generally a pre-incubation time of 1 h at 37°C suffices, when cell permeable compounds are used.
2. The proper amount of protein to load and the dilution range of the primary antibody to use should be assessed in advance in order to establish a linear range of immunodetection for each antibody/antigen pair.
3. If there is too much background staining after visualization, the blocking step can also be performed in 5% BSA solution in TBS±T.
4. Based on the known sequence specificity of the cleavage site for different caspase members, specific substrates have been developed and include Ac-DEVD-AMC for caspases 3 and 7, Ac-LEHD-AMC for caspase 5, Ac-YVAD-AMC for caspases 1 and 4, Ac-IETD-AMC for caspases 8 and 6, and Ac-WEHD-AMC for caspases 1,4, and 5. It should be mentioned, however, that the commercially available substrates, and related FMK inhibitors, do not display restricted specificity. Therefore it is always advisable to combine Western blot assays, for the detection of procaspase processing, with activity assay.
5. In order to detect caspase activity in their natural environment, new tools including activity-based probes, such as CaspACE^{TM} FITC-VAD-FMK In Situ Marker from Promega (Madison, WI, USA), have been developed, which avoid the preparation of lysates and allow a readout of caspase activity state after PDT with minimal interference (Noemi Rubio, personal communication).
6. For quantification of DNA fragmentation during apoptosis a miniaturized (96-well plate format) immunoassays based on the principle of the ELISA (enzyme-linked immunosorbent assay) can also be used. Such assays are commercially available and ensure a high degree of sensitivity. For example, determination of cytoplasmic histone-associated DNA fragments (mono- and oligonucleosomes) using Cell Death Detection ELISA^{PLUS} (Roche Applied Science, Indianapolis, IN, USA) is a useful technique to quantify apoptotic cell death after PDT.
7. The choice of the DNA binding dye is restricted by the absorption and emission spectra of the photosensitizer utilized, which should not overlap.

8. As an alternative method to this Step 3, lysis of the plasma membrane can also be performed with Streptolysin O. Streptolysin O is a bacterial protein that will permeabilize the plasma membrane by binding to cholesterol. Due to the lower abundance of cholesterol in the membranes of organelles, the intracellular membranes will retain their integrity. In this case, resuspend the pellet in 150 μl of stabilization buffer with 200 units of Streptolysin O and transfer to fresh eppendorfs. Vortex shortly and incubate the eppendorfs for 30 min at 37°C. Vortex shortly after incubation and centrifuge for 30 min at 700×*g* at 4°C.
9. Essential for the protocol is the use of DiOC6(3) in the range of 30–40 nM concentration. At higher concentrations the dye will accumulate also in the membranes of the Golgi apparatus and the endoplasmic reticulum, and it is therefore not longer displaying a specific mitochondrial localization.
10. It should be mentioned that the measurement of $\Delta\psi_m$ may not always be a reliable indicator of IM permeabilization, since a drop in $\Delta\psi_m$ can result from inhibited respiration or from transient openings of the permeability transition pore complex (PTPC), which are not necessarily followed by IM permeabilization. The best technique is the calcein quenching method, which can be employed to measure transient IM permeabilization events. This method relies on the loading of the cells with the fluorescent probe calcein, in its acetoxymethyl ester form, as well as with its quencher, cobalt (Co^{2+}) (22). Calcein diffuses to all subcellular compartments, including mitochondria, whereas Co^{2+} ions are excluded from the mitochondrial matrix because the IM is impermeable to these ions. Therefore, functional mitochondria in healthy cells will be visualized by a punctuate fluorescence signal after confocal fluorescence microscopy, whereas upon transient or permanent IM permeabilization, as observed in different PDT paradigms (4), Co^{2+} enters the mitochondrial matrix and quenches the calcein fluorescence (22).
11. Adherent cells can be trypsinized. However, this procedure should be kept as short as possible as it may cause damage to the original morphology of the cells. One method that helps to circumvent this problem is growing adherent cells on plastic coverslips. A major drawback of the latter approach is that only a small amount of cells per section can be analyzed.
12. After fixation with glutaraldehyde, samples can be stored in 0.1 M sodium cacodylate-buffered (pH 7.4) 7.5% saccharose at 4°C for several days.

13. Reynolds solution should be free of carbon dioxide to prevent formation of $PbCO_3$ deposits. Therefore, always use carbon dioxide-free water and sodium hydroxide (Titrisol). Carbon dioxide-free water is prepared by boiling ultrapure water. After transfer of the boiling water in a separating funnel, a carbon dioxide trap filled with soda lime is connected to the outlet on top of the separating funnel to prevent reinfiltration of fresh carbon dioxide.
14. Interpreting electron microscopy is subjective and it can be difficult to distinguish autophagosomes from lysosomes, endosomes, or other structures in the cell. For example, if mitochondria are swollen or contain precipitates, they can be misinterpreted as autophagosomes. Lipid droplets as well as electron lucent or empty vacuoles are also sometimes incorrectly called autophagic vacuoles. Because these vacuoles have no contents, it is not possible to say whether they are autophagic compartments or some other kind of vacuoles. An additional complication is that maturation of mammalian autophagosomes involves a transition to single-membrane structures (i.e., amphisomes and autolysosomes). Therefore, the presence of a double limiting membrane should not be used as a criterion for the identification of autophagosomes. Sometimes, the limiting membrane of autophagic compartments may not have contrast at all, probably due to lipid extraction during sample preparation.
15. LC3-I is highly susceptible to degradation in the lysis buffer, especially during freeze–thaw cycles. Samples with loading buffer should be made as soon as possible after lysis to prevent degradation of LC3-I.
16. The endogenous expression of LC3 might vary notably between cells of different origin. In our experience it is easier to detect LC3 with the commercially available antibody in cells of murine origin than of human origin. The amount of protein and/or concentration of the antibody used might have to be adapted accordingly.
17. The majority of the antibodies for LC3 detection have a higher affinity for LC3-II. This is probably due to the hydrophobic nature of the protein.
18. If overexpression of GFP-LC3 is contraindicated (e.g., transfection problems or another vector carrying a GFP tag), autophagosomes can also be visualized by immunocytochemical staining for endogenous LC3 (use 1–10 μg/ml ab diluted in 1% BSA with 10% serum).
19. GFP-LC3 tends to aggregate in the cell when expressed at high levels, forming "punctuae" independent of the induction of autophagy. Untreated cells and rapamycin-treated

cells as positive controls should be included in the assay. Furthermore, for the visualization of the GFP-LC3 punctuae a mild expression level of the chimeric construct will generate the best results as it will prevent the GFP-LC3-II punctuae from "fading away" in a strong cytoplasmic staining of LC3-I.

20. To detect the specific removal of PDT-damaged organelles by autophagy, a LC3 co-localization analysis can be performed. Either a fluorescent organelle "tracker" or a marker protein, which is specifically targeted to an organelle, can be used for co-localization studies. The latter case requires that the primary antibodies against the marker protein and LC3 have been raised in a different species and that the corresponding secondary antibodies are labeled with different fluorochromes but raised in the same species to prevent crossreactivity. It is also important to make sure that their absorption and excitation spectra do not overlap with those of hypericin or other photosensitizers used. Alternatively hypericin can be washed out during the staining procedure when using 100% ice-cold methanol as a permeabilization agent instead of Triton X-100.
21. When using BafA1 as an inhibitor of autophagy one has to take into account that BafA1 has apoptosis-inducing effects.
22. When monitoring phosphoproteins by Western blotting, replacement of the blocking buffer by 5% BSA in TBS±T is recommended. BSA will repress the crossreactivity of the phospho-specific antibodies with the phosphoproteins present in the milk powder, resulting in a lower background and an enhanced reactivity of the antibodies with their target proteins.
23. While it is essential to remove Tween from the blocking buffer, it does not confer detection problems if added to the incubation buffer for the antibodies. All traces of Tween will be removed in the final washing step (Step 5) with TBS without Tween.

Acknowledgments

The work in author's laboratory is supported by OT/06/49 grant of the Catholic University of Leuven, by F.W.O grants G.0492.05 and G.0661.09. This chapter presents research results of the IAP6/18, funded by the Interuniversity Attraction Poles

Programme, initiated by the Belgian State, Science Policy Office. Michael Dewaele's research is funded by a Ph.D. grant of the Institute for the Promotion of Innovation through Science and Technology in Flanders (IWT-Vlaanderen). Dr. Wim Martinet is a postdoctoral fellow of the F.W.O. Flanders.

References

1. Kroemer, G., Galluzzi, L., Vandenabeele, P., Abrams, J., Alnemri, E. S. et al. (2008) Classification of cell death: recommendations of the Nomenclature Committee on Cell Death 2009. *Cell Death Differ*, **16**, 3–11.
2. Oleinick, N. L., Morris, R. L., and Belichenko, I. (2002) The role of apoptosis in response to photodynamic therapy: what, where, why, and how. *Photochem Photobiol Sci*, **1**(1), 1–21.
3. Dolmans, D. E., Fukumura, D., and Jain, R. K. (2003) Photodynamic therapy for cancer. *Nat Rev Cancer*, **3**(5), 380–387.
4. Buytaert, E., Dewaele, M., and Agostinis, P. (2007) Molecular effectors of multiple cell death pathways initiated by photodynamic therapy. *Biochim Biophys Acta*, **1776**(1), 86–107.
5. Yorimitsu, T. and Klionsky, D. J. (2007) Eating the endoplasmic reticulum: quality control by autophagy. *Trends Cell Biol*, **17**(6), 279–285.
6. Mizushima, N., Levine, B., Cuervo, A. M., and Klionsky, D. J. (2008) Autophagy fights disease through cellular self-digestion. *Nature*, **451**(7182), 1069–1075.
7. Falk, H., Meyer, J., and Oberreiter, M. (1993) A convenient semisynthetic route to hypericin. *Monatshefte fur Chemie*, **124**(3), 339–341.
8. Assefa, Z., Vantieghem, A., Declercq, W., Vandenabeele, P., Vandenheede, J. R. et al. (1999) The activation of the c-Jun N-terminal kinase and p38 mitogen-activated protein kinase signaling pathways protects HeLa cells from apoptosis following photodynamic therapy with hypericin. *J Biol Chem*, **274**(13), 8788–8796.
9. Agostinis, P., Vantieghem, A., Merlevede, W., and De Witte, P. A. (2002) Hypericin in cancer treatment: more light on the way. *Int J Biochem Cell Biol*, **34**(3), 221–241.
10. Buytaert, E., Callewaert, G., Hendrickx, N., Scorrano, L., Hartmann, D. et al. (2006) Role of endoplasmic reticulum depletion and multidomain proapoptotic BAX and BAK proteins in shaping cell death after hypericin-mediated photodynamic therapy. *FASEB J*, **20**(6), 756–758.
11. Salvesen, G. S. and Riedl, S. J. (2008) Caspase mechanisms. *Adv Exp Med Biol*, **615**, 13–23.
12. van Loo, G., Saelens, X., van Gurp, M., MacFarlane, M., Martin, S. J. et al. (2002) The role of mitochondrial factors in apoptosis: a Russian roulette with more than one bullet. *Cell Death Differ*, **9**(10), 1031–1042.
13. Cummings, M. C., Winterford, C. M., and Walker, N. I. (1997) Apoptosis. *Am J Surg Pathol*, **21**(1), 88–101.
14. Falcieri, E., Gobbi, P., Cataldi, A., Zamai, L., Faenza, I. et al. (1994) Nuclear pores in the apoptotic cell. *Histochem J*, **26**(9), 754–763.
15. Kerr, J. F., Winterford, C. M., and Harmon, B. V. (1994) Apoptosis. Its significance in cancer and cancer therapy. *Cancer*, **73**(8), 2013–2026.
16. Clarke, P. G. (1990) Developmental cell death: morphological diversity and multiple mechanisms. *Anat Embryol (Berl)*, **181**(3), 195–213.
17. Klionsky, D. J., Abeliovich, H., Agostinis, P., Agrawal, D. K., Aliev, G. et al. (2007) Guidelines for the use and interpretation of assays for monitoring autophagy in higher eukaryotes. *Autophagy*, **4**(2), 139–140.
18. Chang, L. and Karin, M. (2001) Mammalian MAP kinase signalling cascades. *Nature*, **410**(6824), 37–40.
19. Woodgett, J. R. (2005) Recent advances in the protein kinase B signaling pathway. *Curr Opin Cell Biol*, **17**(2), 150–157.
20. Hay, N. (2005) The Akt-mTOR tango and its relevance to cancer. *Cancer Cell*, **8**(3), 179–183.
21. Agostinis, P., Buytaert, E., Breyssens, H., and Hendrickx, N. (2004) Regulatory pathways in photodynamic therapy induced apoptosis. *Photochem Photobiol Sci*, **3**(8), 721–729.
22. Bernardi, P., Scorrano, L., Colonna, R., Petronilli, V., and Di, L. F. (1999) Mitochondria and cell death. Mechanistic aspects and methodological issues. *Eur J Biochem*, **264**(3), 687–701.

http://www.springer.com/978-1-60761-696-2

Photodynamic Therapy
Methods and Protocols
Gomer, C.J. (Ed.)
2010, XI, 296 p., Hardcover
ISBN: 978-1-60761-696-2
A product of Humana Press